

Densification of LaGaO₃ at low sintering temperatures via Fe³⁺ substitution at Ga³⁺ site

A. CHANDRASEKARAN

Department of Physics, University Putra Malaysia, 43400 UPM Serdang, Selangor, Malaysia

A.-M. AZAD*

NexTech Materials, Ltd., 120-I Lakeview Plaza Blvd., Worthington, OH 43085

E-mail: azad@nextechmaterials.com

Attempts to achieve near theoretical density in polycrystalline LaGaO₃ compacts using Fe₂O₃ as a dopant have been made. The B-site substituted lanthanum gallates with iron doping ranging from 15 to 55 mole% Fe_{0.15} (Fe₂O₃) were synthesized via solid state reaction using oxide and nitrate precursors and sintered at 1200°C for 24 to 72 h and at 1300°C for 12 to 36 h. Systematic variation in the lattice constants and microstructural aspects was followed as a function of mole fraction of Fe₂O₃. It was found that the parent LaGaO₃ structure could take up as high as 55 mole% of Fe₂O₃ retaining the orthorhombic crystal structure. Compositions containing 35 mole% Fe₂O₃ soaked for 48 h or more at 1200°C and for as low as 12 h at 1300°C resulted in perfectly dense compacts. Bodies containing lower dopant concentrations ($x_{\text{Fe}_2\text{O}_3} \leq 0.25$) were found to have a substantial degree of porosity with good intergranular connectivity, while a significant amount of grain growth and broad grain size distribution was an interesting feature in samples containing mole fractions higher than 0.35. © 2001 Kluwer Academic Publishers

1. Introduction

The perovskite-structured lanthanum gallate, LaGaO₃, together with NdGaO₃ had been projected during the last decade and is continued to be used as an excellent substrate material for deposition of thin films of such materials as YBCO hi-*T_c* superconductors and other optoelectronics [1]. However, the first choice in such an application is to use single crystals which are either expensive or not available all the time in convenient geometry and dimensions. Polycrystalline lanthanum gallate, on the other hand, with near theoretical density would be an excellent and inexpensive substitute to the single crystals in such specialized applications, provided other requirements of thin film depositions are satisfactorily met with. In addition, several recent studies have shown that doped LaGaO₃ is a viable alternative to the high temperature yttria-stabilized zirconia (YSZ) electrolyte in the ceramic solid oxide fuel cells (SOFCs) [2–6]. The highest conductivity of 0.14 Scm⁻¹ at 800°C was obtained for the composition La_{0.8}Sr_{0.2}Ga_{0.85}Mg_{0.15}O_{2.825} sintered at 1430°C [4]. Huang *et al.* [5] reported a conductivity of 0.11 Scm⁻¹ at 800°C in samples derived from sol-gel technique, having the composition La_{0.9}Sr_{0.1}Ga_{0.8}Mg_{0.2}O_{2.85}. These values are comparable to those exhibited by YSZ at temperatures in excess of 1000°C.

In the later applications as well, one of the primary pre-requisites is the highest achievable density

of the solid electrolyte without porosity. To this end, Azad and Er [7] have recently shown that a benign microstructure could be obtained in the composition La_{0.9}Sr_{0.1}Ga_{0.8}Mg_{0.2}O_{2.85} soaked for 6 h at 1400°C. A literature survey would reveal that most of the studies reported so far have concentrated on the Sr-doping (at the La-site) and Mg-doping (at the Ga-site). However, there is one investigation pertaining to the electronic conductivity of Fe- and Cr-substituted La_{0.9}Sr_{0.1}GaO₃ [8]. The results showed that while La_{0.9}Sr_{0.1}GaO₃ had high O²⁻ conductivity, the doped materials (La_{0.9}Sr_{0.1}Ga_{1-x}M_xO₃, where M = Fe or Cr; $x = 0.05$ and 0.20) exhibited high electronic conductivity. Therefore, the significant mix of electronic and ionic conductivity in these doped materials was envisaged to be of use as electrodes in SOFCs. The above mentioned study [8], however, used only two compositions, viz., 5 and 20 mole% of the dopants. Therefore, it does not give a clear picture of the effect that a wider dopant concentration would have on the microstructural and conductivity behavior of the resulting formulations. Moreover, the samples used by these authors were sintered at 1500, 1550 and 1600°C for 4 h, leading to two-phase mixtures with the resultant microstructure showing two different morphologies and grain size distribution.

On the other hand, the choice of using Fe₂O₃ (iron in 3+ oxidation state) in the present work as a doping agent was due to the fact that:

* Author to whom all correspondence should be addressed.

(a) the size of Fe^{3+} and Ga^{3+} ions is nearly the same (0.067 and 0.062 nm, respectively); therefore, minimal effect on the CTE and lattice parameter is envisaged, and

(b) both host and the guest ions being isovalent, there would not be a significant amount of lattice defects created in the lattice.

With this objective in perspective, investigation reported in this communication was carried out, where the B-site dopant concentration was varied over a wide range ($0.15 \leq x_{\text{Fe}} \leq 0.55$). The aim was to study the effect of such a large variation of the dopant concentration on the structural and microstructural behavior of the resulting compositions sintered at temperatures much lower than employed hitherto in this system, which in turn would affect their electrical conductivity.

2. Materials synthesis and characterization

Five doped compositions were synthesized via conventional ceramic route, viz., the solid-state reaction. The compounds $\text{La}(\text{NO}_3)_3 \cdot 6\text{H}_2\text{O}$ (99%, Riedel-De Haen, Seelze-Hannover, Germany), Ga_2O_3 (99.99%, Fluka Chemika, Switzerland), $\text{Fe}(\text{NO}_3)_3 \cdot 9\text{H}_2\text{O}$ and $\text{Sr}(\text{NO}_3)_2$ (both 99%, BDH, Poole, UK) were used as the starting materials. Stoichiometric amounts of the starting components were weighed out and mixed so as to give the targeted composition, viz., $\text{La}_{0.9}\text{Sr}_{0.1}\text{Ga}_{1-x}\text{Fe}_x\text{O}_3$ ($0.15 \leq x \leq 0.55$, x varying in intervals of 0.10) up on calcination and sintering. Each of the powder mixture was ball-milled for 2 h in a polystyrene container with 8 clean and polished zirconia balls in acetone as the milling medium. Room temperature drying under UV lamp for few minutes was used to remove acetone. The dry powder was pressed into discs of 6 mm diameter and 2 mm thickness, using double-end compaction with stainless steel die at about 40 MPa. The discs were calcined first at 800°C for 4 h, crushed, thoroughly ground, pelletized and heated again at 1000°C for 24 h. Phase identification was carried out by powder diffraction on a Philips X-ray machine at room temperature, using monochromatic $\text{Cu K}\alpha$ radiation in the range 10 – 90° (2-theta). The X-ray data were used to derive the d -values (interplanar spacing) in each of the solid solutions, which were then used to compute the lattice parameters and unit cell volumes.

Subsequently, each of the calcined powders was blended with 1 wt.% polyvinyl alcohol (PVA) as binder.

The mixture was oven-dried and cold-pressed again, into cylindrical pellets having diameter 6 mm and thickness 1 mm. The as-pressed pellets were sintered in ambient air at 1200°C (for 24, 48 and 72 h) and at 1300°C (for 12, 24 and 36 h). Density measurements on the green as well the sintered pellets by Archimedes principle helped in estimating the degree of densification up on sintering at a constant temperature for a given soak-time.

Microstructural features of the sintered discs were determined by using a JEOL-6400SM scanning electron microscope (Japan). A uniform thin film of gold was evaporated on the exposed surface by Polaron Coating Machine (UK) to avoid electrostatic charging during microscopic viewing. In some cases, prior to SEM examination, samples were thermally etched to clean the grain boundaries by preferential evaporation of volatile impurities, if any.

3. Results and discussion

The XRD spectra of the doped compositions taken on powders after the first-stage calcination at 800°C for 4 h, did not show the principal peaks belonging to LaGaO_3 system. Therefore, the solid-state reaction at this temperature did not seem to have led to the target compound. However, the principal XRD peaks did appear

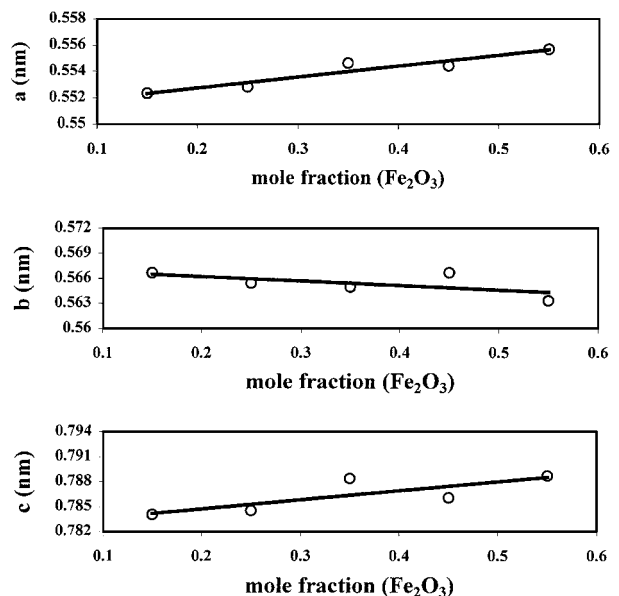
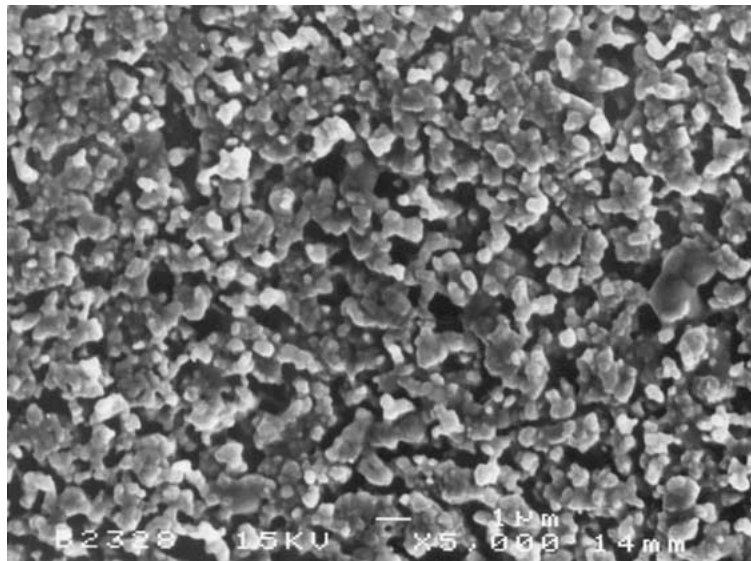


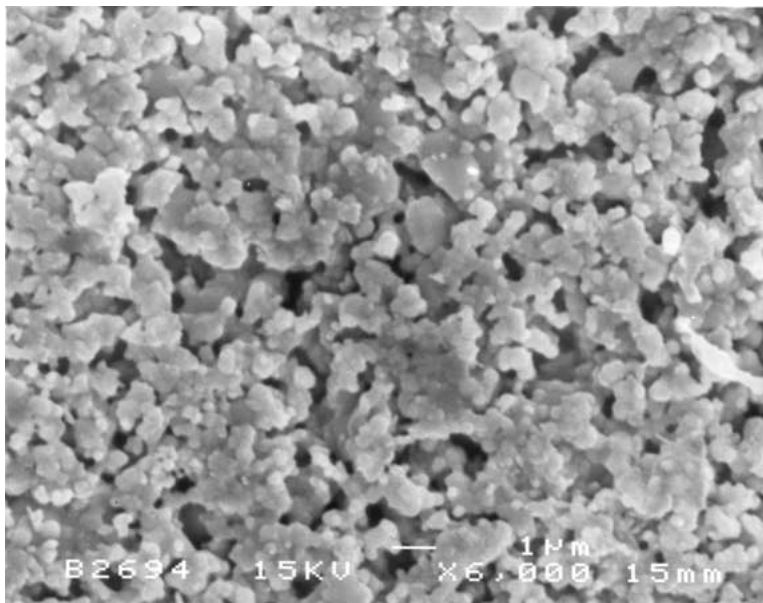
Figure 1 Variation of lattice parameters with mole percent of Fe_2O_3 in LaGaO_3 .

TABLE I Unit cell parameters of $\text{La}_{0.9}\text{Sr}_{0.1}\text{Ga}_{1-x}\text{Fe}_x\text{O}_3$ solid solutions (orthorhombic structure)

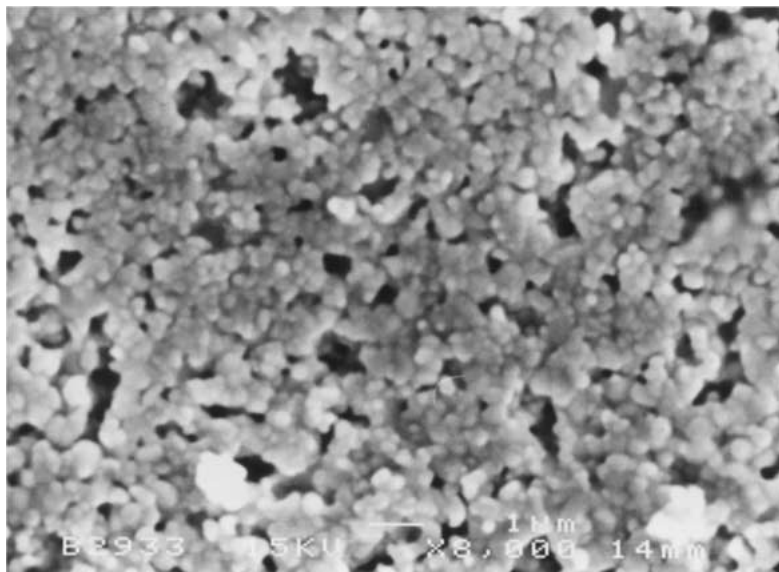
Sample	a/nm	b/nm	c/nm	$V_{\text{cell}}/\text{m}^3$ ($\times 10^{30}$)	Reference
LaGaO_3	.55260	.54730	.77670	230.4700	[11]
LaGaO_3	.55190	.54940	.77000	233.4700	[12]
$\text{La}_{0.9}\text{Sr}_{0.1}\text{Ga}_{0.80}\text{Mg}_{0.20}\text{O}_3$.55215	.55158	.78353	238.6279	[7]
$\text{La}_{0.9}\text{Sr}_{0.1}\text{Ga}_{0.95}\text{Fe}_{0.05}\text{O}_3$.55430	.55420	.78290	240.5000	[8]
$\text{La}_{0.9}\text{Sr}_{0.1}\text{Ga}_{0.80}\text{Fe}_{0.20}\text{O}_3$.55190	.55740	.78440	241.3000	[8]
$\text{La}_{0.9}\text{Sr}_{0.1}\text{Ga}_{0.85}\text{Fe}_{0.15}\text{O}_3$.55236	.56670	.78408	245.4346	This work
$\text{La}_{0.9}\text{Sr}_{0.1}\text{Ga}_{0.75}\text{Fe}_{0.25}\text{O}_3$.55284	.56545	.78456	245.2561	This work
$\text{La}_{0.9}\text{Sr}_{0.1}\text{Ga}_{0.65}\text{Fe}_{0.35}\text{O}_3$.55464	.56499	.78840	247.0578	This work
$\text{La}_{0.9}\text{Sr}_{0.1}\text{Ga}_{0.55}\text{Fe}_{0.45}\text{O}_3$.55440	.56670	.78608	246.9872	This work
$\text{La}_{0.9}\text{Sr}_{0.1}\text{Ga}_{0.45}\text{Fe}_{0.55}\text{O}_3$.55572	.56336	.78872	246.9249	This work



(a)

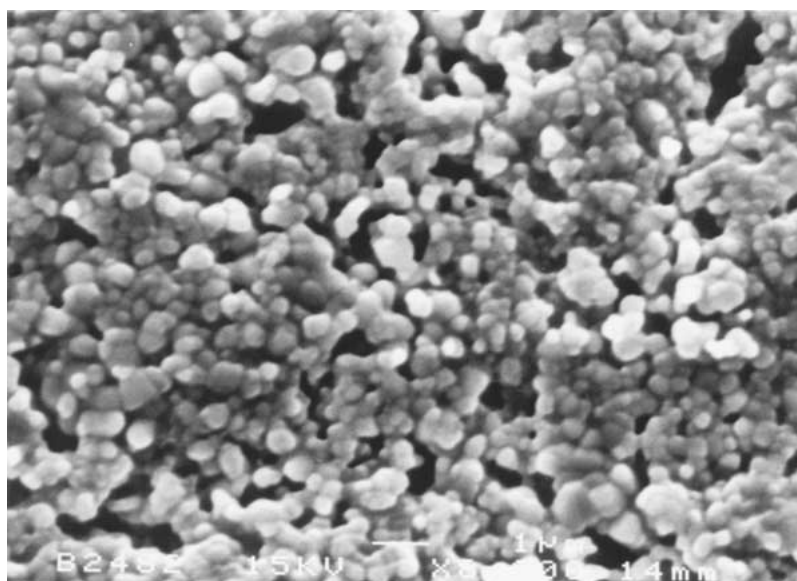


(b)

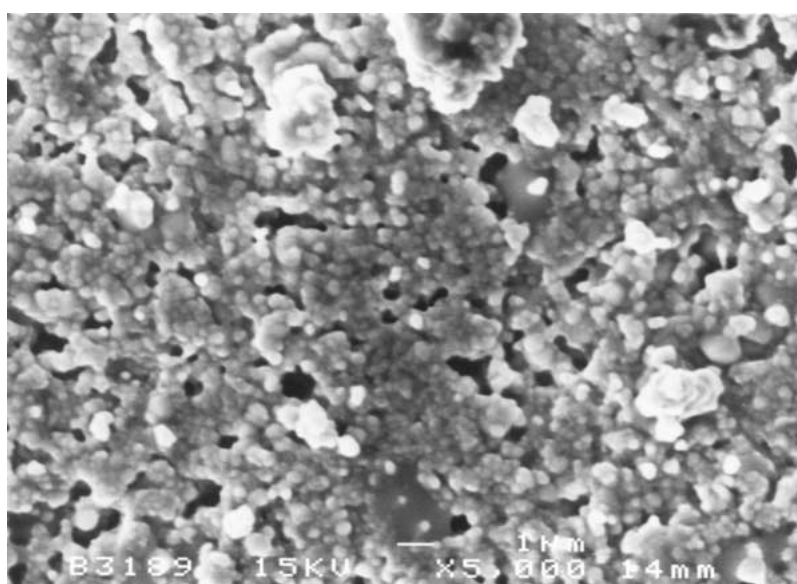


(c)

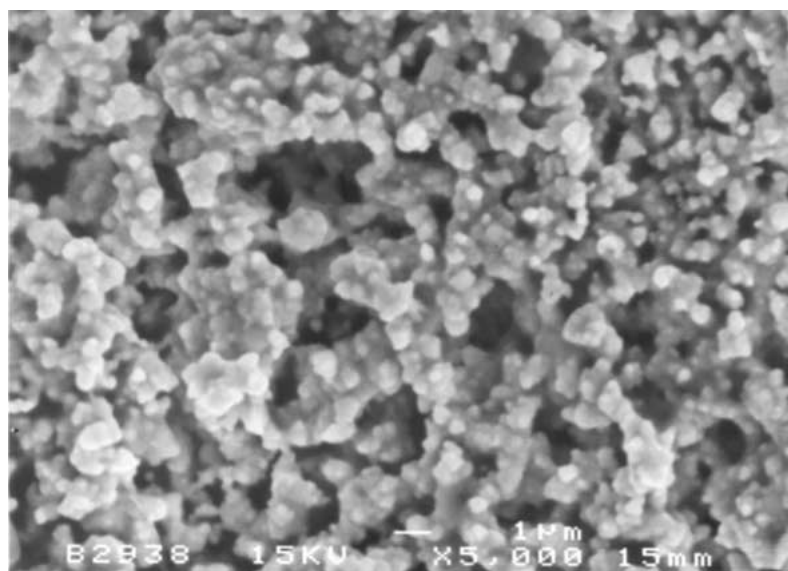
Figure 2 Microstructural evolution after (a) 24 and (b) 48 h soaking in $\text{La}_{0.9}\text{Sr}_{0.1}\text{Ga}_{0.85}\text{Fe}_{0.15}\text{O}_3$ and (c) 72 h soaking of $\text{La}_{0.9}\text{Sr}_{0.1}\text{Ga}_{0.75}\text{Fe}_{0.25}\text{O}_3$ at 1200°C .



(a)

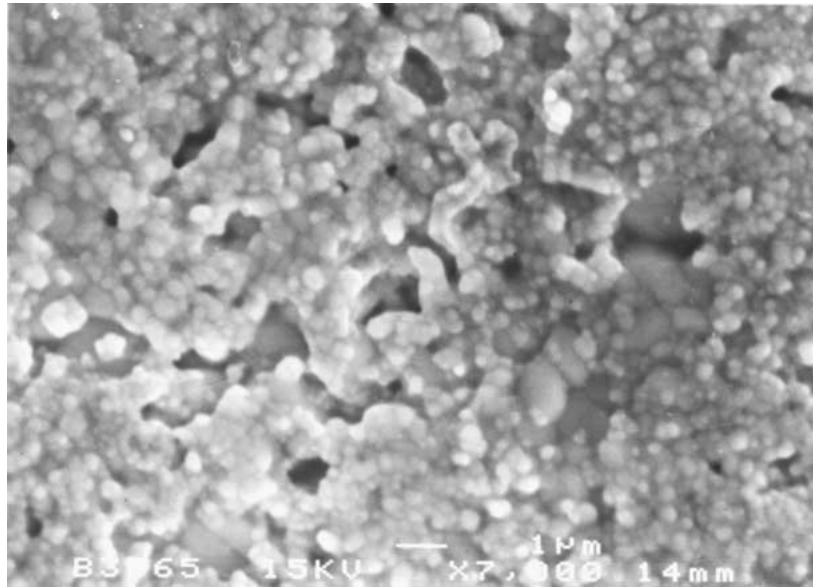


(b)



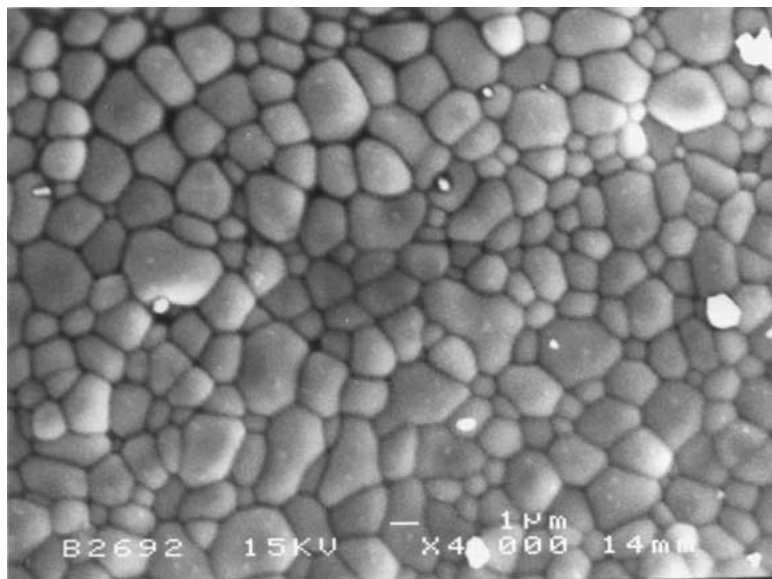
(c)

Figure 3 Microstructural evolution after (a, c) 12 and (b, d) 36 h soaking at 1300°C; (a, b) $\text{La}_{0.9}\text{Sr}_{0.1}\text{Ga}_{0.85}\text{Fe}_{0.15}\text{O}_3$ and (c, d) $\text{La}_{0.9}\text{Sr}_{0.1}\text{Ga}_{0.75}\text{Fe}_{0.25}\text{O}_3$. (Continued.)

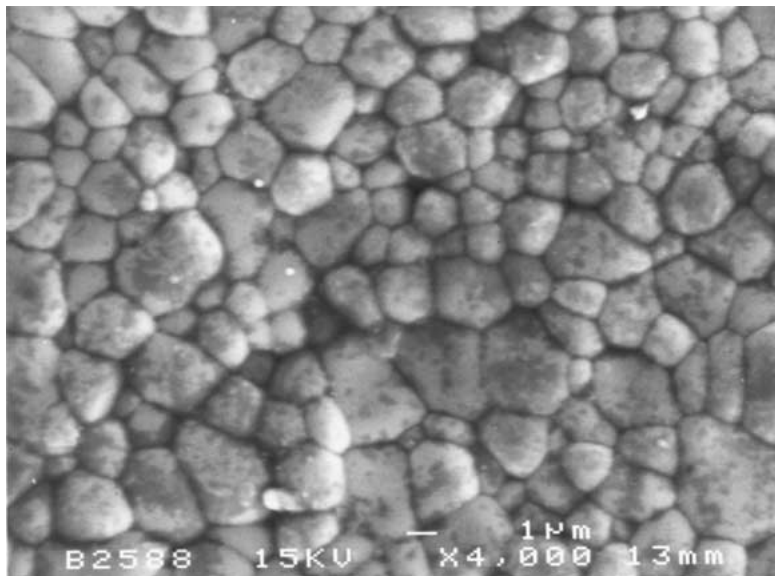


(d)

Figure 3 (Continued.)

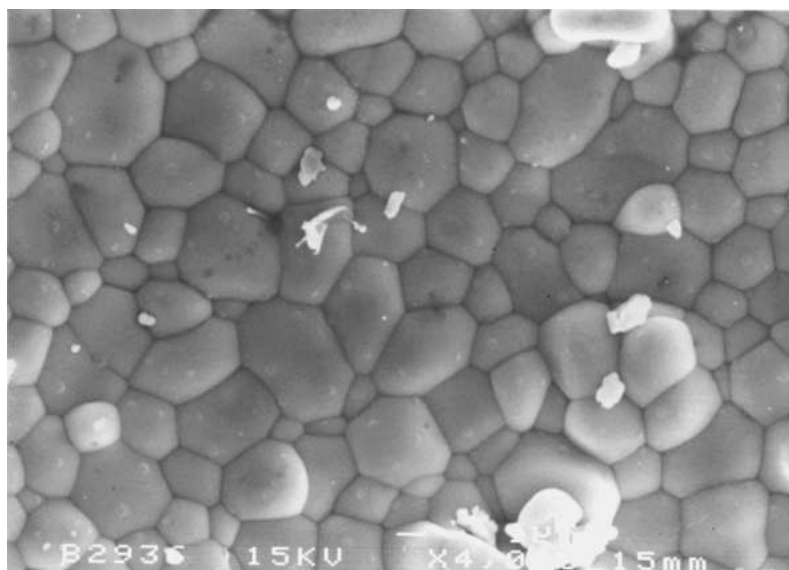


(a)



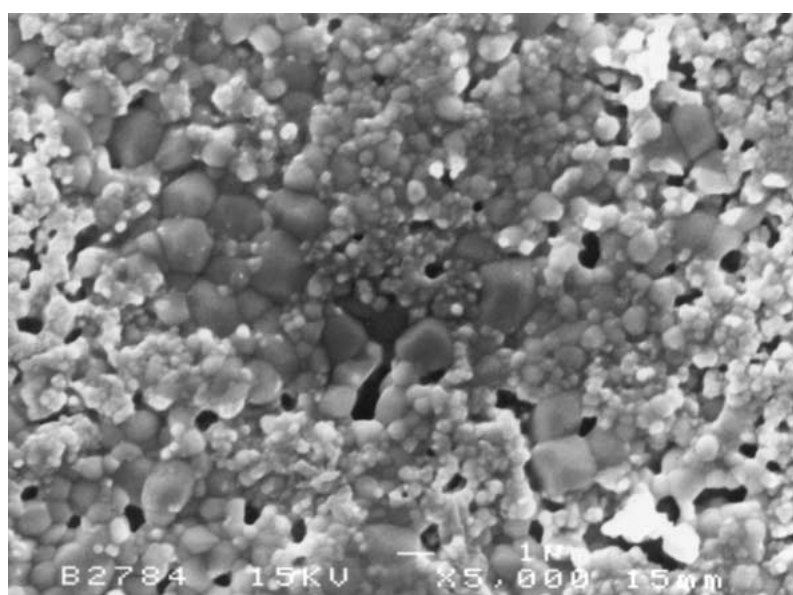
(b)

Figure 4 Microstructure of $\text{La}_{0.9}\text{Sr}_{0.1}\text{Ga}_{0.65}\text{Fe}_{0.35}\text{O}_3$ sintered at for (a) 48 (b) 72 h at 1200°C and (c) 12 h at 1300°C . (Continued.)

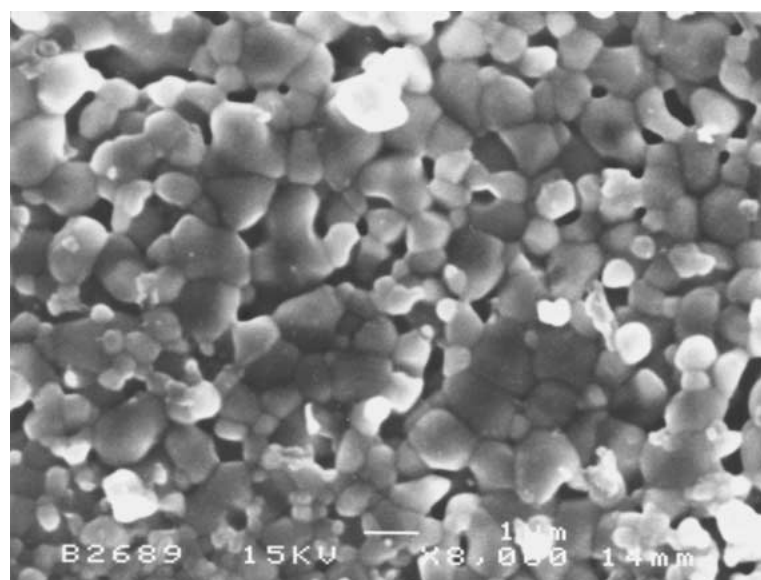


(c)

Figure 4 (Continued.)

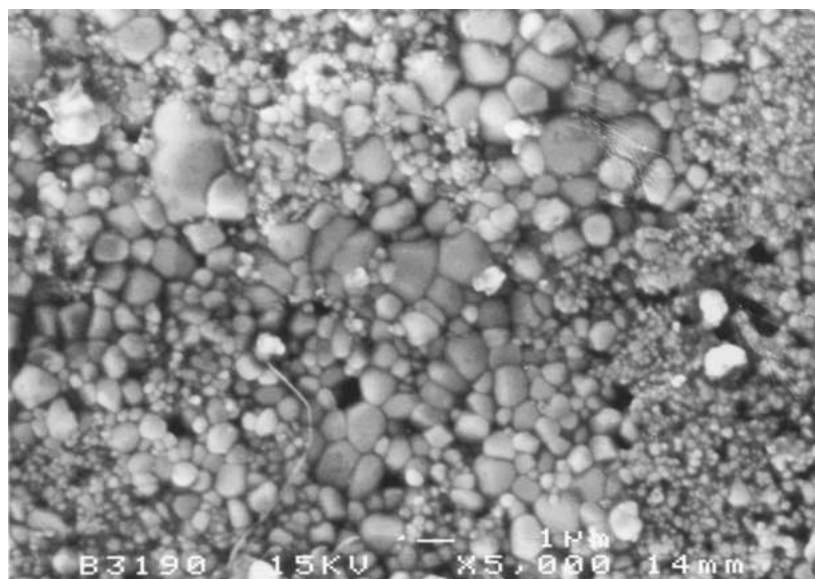


(a)

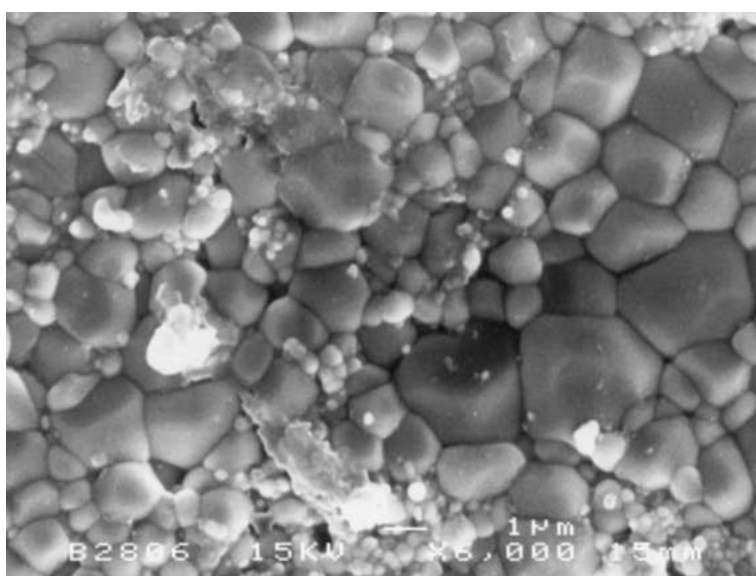


(b)

Figure 5 Microstructural changes in $\text{La}_{0.9}\text{Sr}_{0.1}\text{Ga}_{0.55}\text{Fe}_{0.45}\text{O}_3$ sintered for (a) 24 (b) 48 h at 1200°C and (c) 12 and (d) 24 h at 1300°C . (Continued.)



(c)



(d)

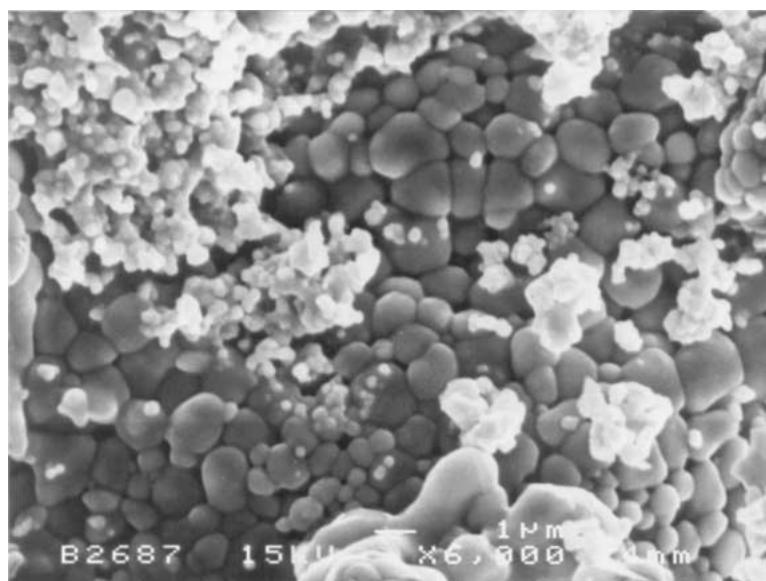
Figure 5 (Continued.)

for all the samples heated at 1000°C for 24 h. From this, it was concluded that the compound formation was complete at 1000°C. This is 100°C lower than that reported by Baker *et al.* [8]. Compound formation at somewhat lower temperature in the present case could be attributed to the use of nitrates (except Ga₂O₃) as the starting materials, instead of oxides. The favorable decomposition kinetics of nitrate precursors, lead to the formation of reactive oxide surfaces upon thermal cleavage. This is very favorable for a facile reaction, leading to the formation of the target compound [9–10].

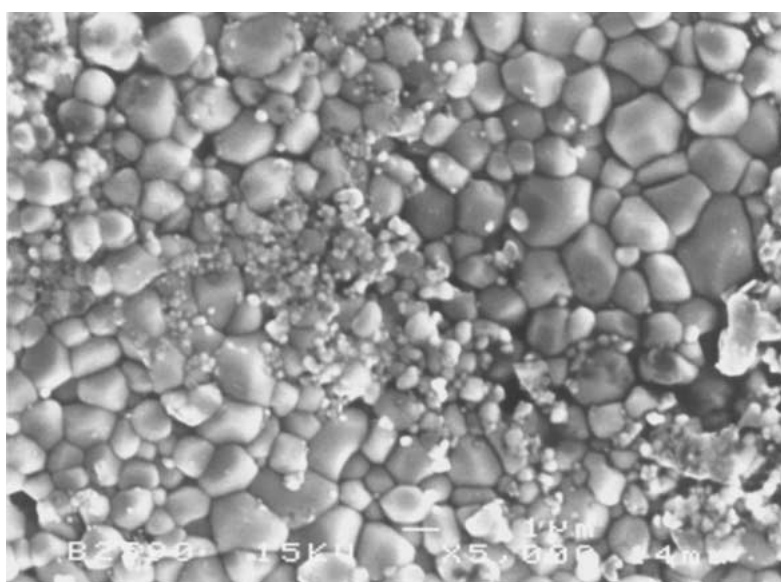
Pure lanthanum gallate, LaGaO₃, crystallizes in orthorhombic modification ($a \neq b \neq c$; $\alpha = \beta = \gamma = 90^\circ$) [11–12]. The ionic radius of Sr²⁺ and Fe³⁺ is slightly larger than that of La³⁺ and Ga³⁺, respectively. Therefore, the lattice parameters of the resulting solid solutions (still in orthorhombic structure) is expected to increase slightly with increasing dopant concentration, assuming the formation of solid solution via substitution. Previous research on La_{0.9}Sr_{0.1}Ga_{1-x}Fe_xO₃

($x = 0.05$ and 0.20) [8] indicated that the principal peak positions in the XRD spectra gave a much better fit to an orthorhombic structure than to a cubic structure, although the latter has been suggested in MgO-doped formulations, La_{1-x}Sr_xGa_{1-y}Mg_yO_{3-δ} ($x = 0.1-0.2$, $y = 0.15-0.25$) [4]. In a recent study on pure and 20 mole% MgO-doped LaGaO₃, Slater *et al.* [13] have shown that at room temperature, the pure and the doped LaGaO₃ crystallize in orthorhombic and pseudo-orthorhombic modification, respectively.

Using the relation of interplanar spacing to cell geometry of a crystalline solid in orthogonal systems, calculations were made to determine the lattice parameters and cell volume of the doped material compositions assuming orthorhombic perovskite structure. The results of these calculations are presented in Table I and shown in Fig. 1. As is seen, the lattice parameters show a monotonic variation when the dopant amount is increased. This suggests that the limit of solid solubility has not been reached in this system even up to



(a)



(b)

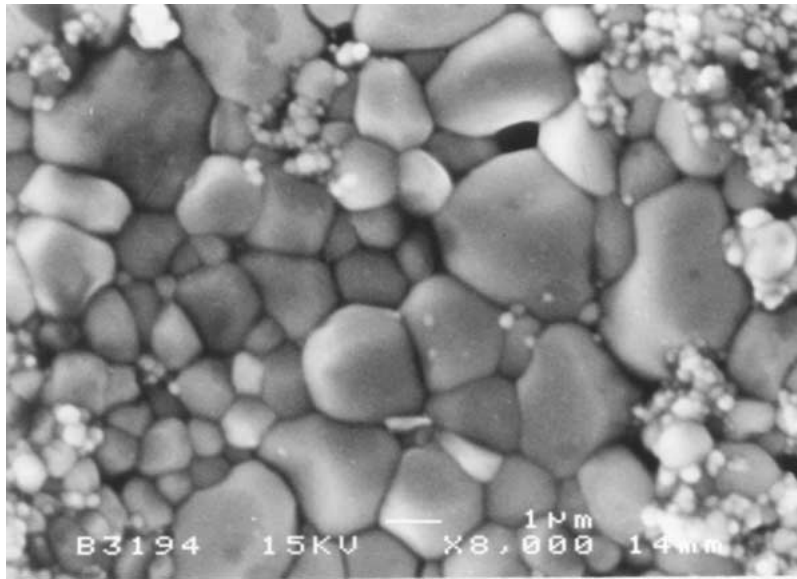
Figure 6 Development of microstructure in $\text{La}_{0.9}\text{Sr}_{0.1}\text{Ga}_{0.45}\text{Fe}_{0.55}\text{O}_3$ sintered at 1200°C for: (a) 48 and (b) 72 h.

55 mole% of Fe_2O_3 , though there is a slight increase in the cell parameter 'c' for 35 and 55 mole% Fe_2O_3 doping.

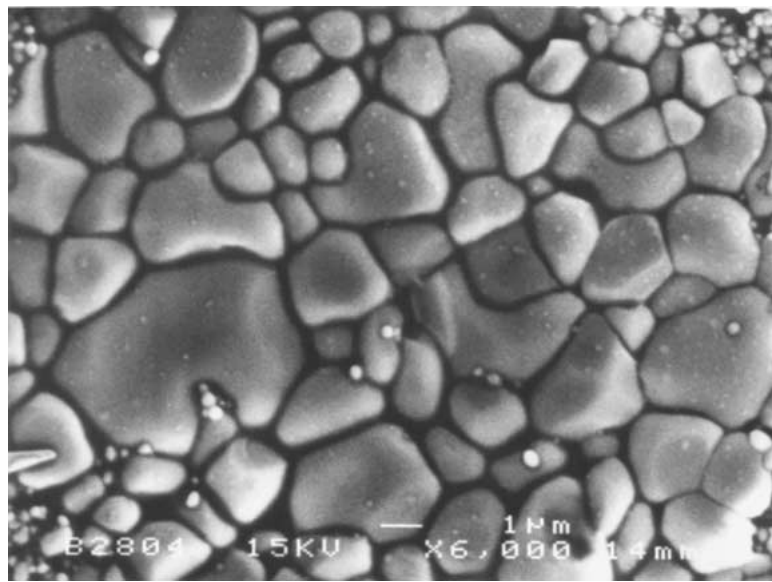
Examination of the microstructural features evolved in sintered samples revealed interesting systematic both with respect to the dopant concentration and the sintering conditions. For example, the compacts doped with 15 and 25 mole% Fe_2O_3 and soaked up to 72 h at 1200°C , retained a significant amount of porosity (density up to $\sim 70\%$ theoretical) without any noticeable grain growth (average grain size $< 1 \mu\text{m}$). This is typically shown in Fig. 2(a–c), where a systematic increase in intergranular connectivity (but without any perceptible grain growth) with longer soak-time could be easily made out. Up on raising the sintering temperature to 1300°C for the compacts with compositions in the same range, the morphological features did not alter much except for slightly better grain-to-grain connectivity, leading to higher density ($\sim 81\%$ theoretical). This is illustrated in Fig. 3(a–d).

The microstructures shown in Fig. 4 were obtained on 35 mole% Fe_2O_3 -doped samples subsequent to their sintering at 1200 and 1300°C for various duration. As can be seen from these micrographs, very high densification ($\sim 99\%$ theoretical) could be achieved even at $1200^\circ\text{C}/48 \text{ h}$. The average grain size is $1\text{--}2 \mu\text{m}$ in samples soaked at 1200°C , whereas it is $\sim 2 \mu\text{m}$ in samples sintered at 1300°C . The grain size distribution, however, is much narrower in samples exposed to 1300°C .

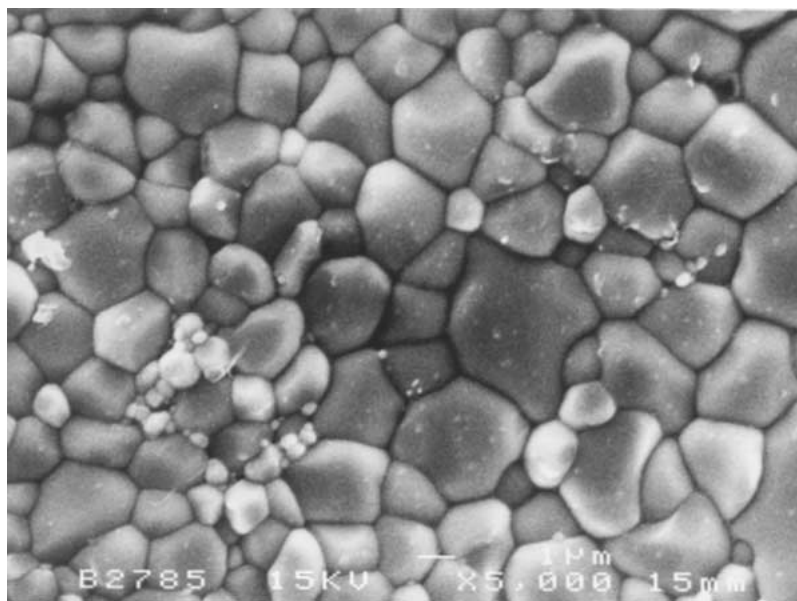
The porous features observed in samples containing $x_{\text{Fe}_2\text{O}_3} < 0.35$ are again seen in compacts containing higher than 0.35 mole% of Fe_2O_3 . Fig. 5 shows the microstructural evolution in sintered samples doped with 45 mole% of Fe_2O_3 . Sintering at 1200°C for 24 h (Fig. 5a) improved the densification (evidenced by isolated porosity of small volume) accompanied by grain growth in some regions. Two sets of grains with distinct dimensions could readily be recognized: one, agglomerated sub-micron sized particles and the other with sharp geometrical features having excellent



(a)



(b)



(c)

Figure 7 Development of microstructure in $\text{La}_{0.9}\text{Sr}_{0.1}\text{Ga}_{0.45}\text{Fe}_{0.55}\text{O}_3$ sintered at 1300°C for: (a) 12 (b) 24 (c) 36 h.

grain-to-grain connectivity and about $\sim 1 \mu\text{m}$ in size. Increase in soak time to 48 h (Fig. 5b) caused significant grain growth and intergranular connectivity without affecting the porosity significantly. However, when the soak time was increased to 72 h, the amount of porosity is seen to increase significantly with reduction in grain size. This could be attributed to the competing phenomenon of mass transport with grain growth at longer soak-times.

The behavior of the sample sintered at 1300°C between 12 to 36 h was similar to that observed in samples sintered at 1200°C . In samples soaked for 12 h (Fig. 5c), isolated pockets of grain growth could be seen while grains of sub-micron size were still present. Increasing the soak time to 24 h led to significantly high degree of densification and grain growth (Fig. 5d). Some of the grains were as big as $3 \mu\text{m}$. However, when the soak time was increased to 36 h the porosity also increased, the latter still remaining non-connected and isolated.

Sintering of samples doped with 55 mole% of Fe_2O_3 at 1200°C for 24 and 48 h led to a small fraction of abnormal grain growth. Increasing the soak time to 72 h led to much enhanced densification ($\sim 88\%$ theoretical), though still showing the presence of sub-micron sized grains (Fig. 6). On the other hand, sintering at 1300°C in the range 12 to 36 h led to a highly densified microstructure with significant grain growth (grain size of the order of 2 to $5 \mu\text{m}$). This is shown in Fig. 7, where a rather broad grain size distribution could be readily recognized.

It should be pointed out that though Baker *et al.* [8] measured the impedance of 5 and 20 mole% Fe_2O_3 -doped LaGaO_3 , they reported the microstructures of 5 mole% Fe_2O_3 -doped composition alone. Sintering was done at 1500° , 1550° and 1600°C for 4 h each. These temperatures being rather high, the resulting microstructures were undoubtedly dense and granular. Wide grain size distribution, however, was visible only in samples sintered at 1600°C , while those sintered at lower temperatures still contained an appreciable degree of porosity. In contrast to that, the present investigation revealed that sintering at 1200 – 1300°C was adequate to yield highly dense morphology. The ease of sintering and excellent densification with appropriate grain size (more significantly in the case of formulation containing 35 mole% Fe_2O_3) at relatively lower temperatures employed in the present investigation, could be attributed to the possible formation of LaFeO_3 —an excellent electronic conductor. Though the XRD signatures of the powders did not suggest the presence of this phase, it is likely that it was formed in trace amounts, beyond the level of detection by XRD technique. This phase, if formed at the grain boundaries, could create defect states, thereby promoting densification. Another

possibility is that a concurrent reaction leading to the formation of $\text{La}_{0.9}\text{Sr}_{0.1}\text{FeO}_{2.90}$ phase (again in small amount) could have taken place. Formation of such a phase with oxygen non-stoichiometry is likely to participate in sintering process in a benign fashion. More experiments, however, are warranted to confirm this speculation, using sensitive analytical tools.

4. Conclusions

Five doped formulations with iron doping at B-site in $\text{La}_{0.9}\text{Sr}_{0.1}\text{GaO}_3$ between 15 and 55 mole% were synthesized via solid-state reaction technique. The sintered bodies were characterized by structural and microscopic means. In the light of these results, it may be concluded that:

(i) There seems to be an optimum dopant concentration to arrive at the most benign dense microstructure in Fe_2O_3 -doped LaGaO_3 system; in the present case, it appears to be 35 mole% Fe_2O_3 .

(ii) Samples containing 35 mole% Fe_2O_3 sintered at 1200°C for the duration $48 \text{ h} \leq t \leq 72 \text{ h}$ and those sintered at 1300°C for 12 h showed systematic grain growth and densification.

(iii) Formation of LaFeO_3 and/or $\text{La}_{0.9}\text{Sr}_{0.1}\text{FeO}_{2.90}$ phase could have accelerated the densification and grain growth process in compositions with higher than 35 mole% dopant concentration, leading to abnormal grain growth and larger grain size distribution.

References

1. A.-M. AZAD, S. SUDHA and O. M. SREEDHARAN, *Mater. Res. Bull.* **26** (1991) 97.
2. T. ISHIHARA, H. MATSUDA and Y. TAKITA, *J. Am. Chem. Soc.* **116** (1994) 3801.
3. *Idem.*, *Solid State Ionics* **79** (1995) 147.
4. (a) P. N. HUANG and A. PETRIC, *J. Mater. Chem.* **5** (1995) 53; (b) *Idem.*, *J. Electrochem. Soc.* **143** (1996) 1644.
5. K. HUANG, M. FENG and J. B. GOODENOUGH, *J. Amer. Ceram. Soc.* **79** (1996) 1100.
6. K. HUANG, R. S. TICHY and J. B. GOODENOUGH, *ibid.* **81** (1998) 2565.
7. A.-M. AZAD and L. F. ER, *J. Alloys Comp.* **306** (2000) 103.
8. R. T. BAKER, B. GHARBAGE and F. M. B. MARQUES, *J. Europ. Ceram. Soc.* **18** (1998) 105.
9. A.-M. AZAD and N. C. HON, *J. Alloys Comp.* **270** (1998) 95.
10. A.-M. AZAD, L. L. W. SHYAN and P. T. YEN, *ibid.* **282** (1999) 109.
11. M. MAREZIO, J. P. REMIKA and P. D. DERNIER, *Mater. Res. Bull.* **1** (1966) 247.
12. S. GELLER, P. J. CURLANDER and G. F. RUSE, *ibid.* **9** (1974) 637.
13. P. R. SLATER, J. T. S. IRVINE, T. ISHIHARA and Y. TAKITA, *J. Solid State Chem.* **139** (1998) 135.

Received 1 June 2000

and accepted 31 May 2001